

Prognostic Value of Right Ventricle–Pulmonary Artery Uncoupling in Transthyretin Amyloidosis

Valor pronóstico del desacoplamiento ventrículo derecho-arteria pulmonar en la amiloidosis por transtiretina

JAQUELINE FREYRE HERNANDO¹, ANA SPACCAVENTO¹, LUCRECIA BURGOS^{1, MTSAC}, IVANA SEIA¹, ALAN SIGAL^{1, MTSAC}, PABLO ELISSAMBURU^{1, MTSAC}, MIRTA DIEZ^{1, MTSAC}, MARTÍN VIVAS^{1, MTSAC}, JUAN P COSTABEL^{1, MTSAC}.

ABSTRACT

Background: Right ventricular involvement is a common manifestation of transthyretin cardiac amyloidosis (ATTR-CA), especially in advanced stages, and may have significant prognostic implications. Echocardiographic assessment of the right ventricle (RV), however, remains challenging. In this context, the relationship between tricuspid annular plane systolic excursion (TAPSE) and systolic pulmonary artery pressure (SPAP), as well as the relationship between tissue Doppler S wave (S'TDI) and SPAP, have been proposed as markers of RV-pulmonary artery (RV-PA) uncoupling, which could more accurately reflect the functional load on the RV. **Objective:** The aim of this study was to analyze the prognostic value of TAPSE/SPAP and S'TDI/SPAP ratios in patients with ATTR-CA, and to compare them with other traditional clinical and echocardiographic predictors regarding the risk of hospitalization for heart failure (HHF).

Methods: A retrospective analysis was performed of patients with confirmed diagnosis of ATTR-CA under outpatient follow-up at a cardiomyopathy clinic. Clinical, biochemical, and echocardiographic data were collected at the time of diagnosis, and events of HHF were documented during follow-up. The primary outcome was the first HHF. Univariate and multivariate Cox regression models were applied to identify independent predictors, and Kaplan-Meier analysis were used to evaluate event-free survival curves. The optimal cut-off points for continuous variables were defined by Youden's index.

Results: A total of 191 patients (mean age 80 ± 7.9 years, 88.5% men) were included, all with preserved or mildly reduced left ventricular ejection fraction, with a median value of 53% and interquartile range (IQR) 43-61, and echocardiographic evidence of RV dysfunction, with median TAPSE 18 mm (IQR 15–20) and S'TDI 9.5 (IQR 8–10). During a median follow-up of 391 days (IQR 84–704), 32% of patients had at least one HHF. In the univariate analysis, a higher TAPSE/SPAP ratio was associated with lower risk of hospitalization (HR 0.149; $p = 0.039$), as were higher TAPSE values alone (HR 0.959; $p=0.040$) and older age (HR 1.066; $p=0.010$), while SPAP alone was not significant (HR 1.014; $p=0.100$). In the multivariate analysis, a TAPSE/SPAP ratio ≤ 0.5 (optimal cutoff point with 78% sensitivity, 67% specificity, and area under the ROC curve 0.60) was independently associated with a higher risk of hospitalization (HR 2.05; 95% CI 1.10–4.33; $p = 0.025$). In contrast, the S'TDI/SPAP ratio showed no independent association ($p = 0.843$).

Conclusions: In patients with ATTR-CA, RV–PA uncoupling, estimated by a TAPSE/SPAP ratio ≤ 0.5 , is associated with an increased risk of HHF, even with preserved ejection fraction. Conversely, the S'TDI/SPAP ratio did not provide prognostic value. Due to its simplicity and availability, the TAPSE/SPAP ratio could be incorporated as a complementary risk stratification tool in this population.

Key words: Cardiac amyloidosis - Right ventricle - TAPSE - Pulmonary systolic pressure - Tissue Doppler – Hospitalization - Heart failure

RESUMEN

Introducción: La afectación del ventrículo derecho (VD) es una manifestación frecuente en la amiloidosis cardíaca por transtiretina (CA-TTR), especialmente en etapas avanzadas, y puede tener implicancias pronósticas relevantes. La evaluación ecocardiográfica del VD, sin embargo, continúa siendo desafiante. En este contexto, la relación entre el desplazamiento sistólico del anillo tricúspideo (TAPSE) y la presión sistólica de la arteria pulmonar (PSAP), así como la relación de la onda S por Doppler tisular (S'TDI) y la PSAP, han sido propuestas como marcadores del desacoplamiento VD-arteria pulmonar (VD-AP), lo que podría reflejar con mayor precisión la carga funcional del VD.

Objetivo: Analizar el valor pronóstico de las relaciones TAPSE/PSAP y S'TDI/PSAP en pacientes con CA-TTR, y compararlas con otros predictores clínicos y ecocardiográficos tradicionales, en relación con el riesgo de hospitalización por insuficiencia cardíaca (HIC).

REV ARGENT CARDIOL 2026;94:46-54. <https://doi.org/10.7775/rac.v94.i1.20969>

Received: 11/05/2025 – Accepted: 12/17/2025

Correspondence: Juan Pablo Costabel. Instituto Cardiovascular de Buenos Aires (ICBA). Av. del Libertador 6302, CP 1428, Autonomous City of Buenos Aires, Argentina. Email: jpcostabel@icba.com.ar

This article won the Dr. Oscar Orias Runner-up Prize at the 51st Argentine Congress of Cardiology.



<https://creativecommons.org/licenses/by-nc-sa/4.0/>

©Revista Argentina de Cardiología

¹ Cardiomyopathy Clinic at Instituto Cardiovascular de Buenos Aires (ICBA), Buenos Aires, Argentina.

Material y métodos: Se realizó un análisis retrospectivo de pacientes con diagnóstico confirmado de CA-TTR bajo seguimiento ambulatorio en una clínica especializada en miocardiopatías. Se recolectaron datos clínicos, bioquímicos y ecocardiográficos al momento del diagnóstico, y se documentaron eventos de HIC durante el seguimiento. El desenlace primario fue la primera hospitalización por IC. Se emplearon modelos de regresión de Cox univariado y multivariado para identificar predictores independientes, y análisis de Kaplan Meier para evaluar curvas de supervivencia libre de eventos. Los puntos de corte óptimos de las variables continuas se definieron por el índice de Youden.

Resultados: Se incluyeron 191 pacientes (edad media $80 \pm 7,9$ años, 88,5 % hombres), todos con fracción de eyección del ventrículo izquierdo preservada o levemente reducida, con mediana 53% y rango intercuartílico (RIC) 43-61, y evidencia ecocardiográfica de disfunción del VD, con medianas de TAPSE 18 mm (RIC 15-20), y onda S'-TDI 9,5 (RIC 8-10). Durante un seguimiento mediano de 391 días (RIC 84–704), 32 % de los pacientes presentó al menos una hospitalización por IC. En el análisis univariado una mayor relación TAPSE/PSAP se asoció con menor riesgo de hospitalización (HR 0,149; $p = 0,039$), al igual que valores más altos de TAPSE de forma aislada (HR 0,959 $p=0,040$) y mayor edad (HR 1,066; $p=0,010$), mientras que la PSAP aislada no fue significativa (HR 1,014; $p=0,100$). En el análisis multivariado, una relación TAPSE/PSAP $\leq 0,5$ (punto de corte óptimo con sensibilidad 78 %, especificidad 67 % y área bajo la curva ROC 0,60) se asoció de manera independiente con mayor riesgo de hospitalización (HR 2,05; IC95 % 1,10–4,33; $p = 0,025$). En contraste, la relación S'TDI/PSAP no mostró asociación independiente ($p = 0,843$).

Conclusiones: En pacientes con CA-TTR, el desacoplamiento VD-AP, estimado por una relación TAPSE/PSAP $\leq 0,5$, se asocia con mayor riesgo de HIC, aun con fracción de eyección preservada. En contraste, la relación S'TDI/PSAP no aportó valor pronóstico. La relación TAPSE/PSAP, por su simplicidad y disponibilidad, podría incorporarse como herramienta complementaria de estratificación de riesgo en esta población.

Palabras clave: Amiloidosis cardíaca - Ventrículo derecho - TAPSE - Presión sistólica pulmonar - Doppler tisular - Hospitalización - Insuficiencia cardíaca.

INTRODUCTION

Transthyretin cardiac amyloidosis (ATTR-CA) is an infiltrative disease characterized by the extracellular deposition of this misfolded protein fibers in the myocardium. This process leads to increased wall thickness, ventricular stiffness, and, in the early stages, relative preservation of left ventricular (LV) systolic function. (1–4) With progression, elevated filling pressures, atrial remodeling, and secondary pulmonary hypertension are observed, with right ventricular (RV) overload. (5)

Right ventricular dysfunction in ATTR-CA has been associated with an increased risk of hospitalization and mortality, regardless of left ventricular function. (6,7) In this context, the RV ability to adapt to pulmonary circulation may be compromised by pressure overload and progressive myocardial stiffness, favoring the development of right ventricle–pulmonary artery (RV–PA) uncoupling. (8)

RV–PA coupling describes the interaction between ventricular contractility and pulmonary afterload. Its echocardiographic assessment using the ratio of tricuspid annular plane systolic excursion (TAPSE) to systolic pulmonary artery pressure (SPAP) has proven to be a simple and noninvasive index, with good correlation with invasive measurements. (9,10) In heart failure and pulmonary hypertension, this parameter has been established as a clinical and prognostic marker. (11–15) However, in cardiac amyloidosis, the evidence remains limited and expanding. (16–19)

On the other hand, tricuspid annulus S' wave velocity obtained by tissue Doppler imaging (S'TDI) is a sensitive parameter of RV longitudinal systolic function, with good correlation with ejection fraction measured by magnetic resonance imaging (20). However, its application in RV–PA coupling indices, such as the S'TDI/SPAP ratio, still lacks clinical validation in ATTR-CA.

In this context, the present study aimed to evaluate the prognostic value of RV–PA uncoupling in patients with ATTR-CA, estimated by the TAPSE/SPAP ratio, and to explore the usefulness of the S'TDI/SPAP ratio in predicting hospitalization for heart failure (HHF).

METHODS

Study design and population

A retrospective, single-center observational cohort study was conducted using data obtained prospectively from electronic medical records. Patients followed up on an outpatient basis at the institution's Cardiomyopathy Clinic between January 2011 and March 2025, with a diagnosis of ATTR-CA according to the diagnostic criteria in force during that period, were included. (21)

Demographic data (age, sex), clinical history, cardiovascular risk factors, and baseline echocardiographic parameters were recorded. Patients were followed up for clinical events, and their data were recorded in a database specific for the disease.

Confirmation of transthyretin cardiac amyloidosis

The diagnosis was established based on echocardiographic findings typical of infiltrative cardiomyopathy (LV wall thickness ≥ 12 mm) and grade 2 or 3 myocardial uptake on bone scintigraphy with technetium-99m hydroxymethylene diphosphonate (99mTc-HMDP, The Binding Site, Birmingham, UK), together with the exclusion of clonal dyscrasia by serum and urinary immunofixation and free light chain assay (Freelite, The Binding Site, Birmingham, UK). (4)

The scintigraphy was performed with 20 mCi of 99mTc-HMDP administered intravenously, acquiring flat images after 2 hours. Semiquantitative cardiac uptake relative to bone tissue was evaluated using the Perugini scale (0–3) and quantitative assessment was performed using the heart/lung ratio.

The final diagnosis of ATTR-CA was established by integrating the clinical evaluation with electrocardiographic, echocardiographic, and scintigraphy data, after excluding light chain (AL) disease (free light chains, serum and urinary immunofixation). (22,23) Gadolinium enhanced magnetic resonance imaging was indicated in selected cases, and

when diagnostic doubts persisted, a tissue biopsy was performed.

Echocardiography

Transthoracic echocardiograms (TTE) obtained in a stable clinical situation, corresponding to the time closest to the amyloidosis diagnosis, were retrieved and reanalyzed.

Images were acquired using Philips iE33 and HD15 ultrasound machines, and in subsequent years Philips EPIQ 7 and Affinity (Philips Medical Systems, Andover, MA, USA). Post-processing was performed independently by a trained cardiologist using QLAB and UniViewer workstations (Philips Medical Systems, Andover, MA, USA).

Measurements followed the recommendations of the American Society of Echocardiography (ASE) and the European Association of Cardiovascular Imaging (EACVI) for chamber quantification, ventricular function assessment, and pulmonary pressure estimation. (24,25)

The following measurements were obtained:

- TAPSE: tricuspid annular plane systolic excursion in M-mode (mm).
- S'TDI: longitudinal systolic velocity of the RV by pulsed tissue Doppler in the tricuspid annulus (cm/s).
- SPAP: calculated as $4 \times (\text{maximum tricuspid regurgitation velocity})^2 + \text{right atrial pressure}$, estimated by inferior vena cava diameter and collapsibility (mmHg).
- LVEF: left ventricular ejection fraction, using Simpson's biplane method in 4- and 2-chamber apical projections (%).

Based on these variables, the RV-PA coupling indices were calculated: TAPSE/SPAP and S'TDI/SPAP.

Outcome and follow-up

The primary outcome was time to first HHF, defined as hospitalization ≥ 24 h for documented signs/symptoms of congestion with intensified treatment (IV diuretics and/or vasodilators/inotropic drugs)

Time 0 was defined as the date of baseline TTE (the study closest to diagnosis in a stable situation). Patients without an event were censored on the date of last documented contact or death without prior HHF. Follow-up duration was reported as median and interquartile range (IQR).

Statistical analysis

Continuous variables were presented as mean \pm standard deviation (SD) or median and IQR according to their distribution (assessed with the Shapiro-Wilk test); homogeneity of variances was verified with the Levene test. For univariate comparisons, Student's *t* or Mann-Whitney *U* (for continuous variables) and χ^2 or Fisher (for categorical variables) tests were used, as appropriate.

The association between echocardiographic parameters and the primary outcome was evaluated using univariate and multivariate Cox proportional hazards models, reporting hazard ratios (HR) with their 95% confidence intervals (95% CI). The number of predictors in the multivariate model was limited by the approximate rule of ~ 10 events per predictor.

The discriminatory capacity of the RV-PA uncoupling indices (TAPSE/SPAP and S'TDI/SPAP) was analyzed using ROC curves with area under the curve (AUC) and 95% CI (DeLong method). The optimal cutoff point for TAPSE/SPAP was determined using the Youden index. Kaplan-Meier curves stratified by cutoff point were built and compared using the log-rank test. A *p*-value < 0.05 was considered significant.

The analyses were performed for complete cases using IBM SPSS Statistics version 29.0.

Ethical considerations

The protocol was approved by the institutional Ethics Committee. Informed consent was waived given the retrospective nature and the use of anonymized data. The study was conducted in accordance with the Declaration of Helsinki (26) and national regulations (Resolution 1480/2011 of the National Ministry of Health, Law 3301 of the City of Buenos Aires, and Resolution 6677/10 of ANMAT and its 4008 and 4009 amendments).

RESULTS

Study population (Table 1)

Between January 2011 and March 2025, 228 patients were evaluated and 37 were excluded (due to single TTE during hospitalization for decompensated HF, *n* = 16; no TTE or not performed at our institution, *n* = 7, TTE without sufficient data to assess SPAP, *n* = 14), leaving 191 for analysis (Figure 1).

Mean age was 80 ± 7.9 years, and 88.5% were men. Functional class at the time of baseline TTE was predominantly NYHA I in 62 patients (32.4%) and II in 100 (52.4%). The most frequent comorbidities were hypertension in 131 cases (68.8%) and dyslipidemia in 104 (54.5%). Among the "red flags" for ATTR-CA, carpal tunnel syndrome was observed in 55 patients (27.2%), neuropathy in 11 (5.4%), and spinal stenosis in 12 (5.9%). Atrial fibrillation was present in 93 cases (46.0%) and developed during follow-up in 26 (12.9%). The remaining baseline characteristics are shown in Table 1.

Echocardiographic parameters and RV-PA coupling (Table 2)

In baseline echocardiography, median LVEF was 53% (IQR 43–61) with verified increased LV wall thickness. Median left atrial area was 28 cm² (25–33). Pseudonormal, restrictive, and monophasic wave mitral filling patterns predominated; median mitral E wave and tissue *e'* ratio (*E/e'*) was 14 (IQR 10–18); TAPSE was 18 mm (15–20), and tricuspid annulus S'TDI was 9.5 cm/s (8–10). SPAP reached 38 mm Hg (31–48). The RV-PA coupling indices were 0.43 (0.32–0.62) for the TAPSE/SPAP ratio and 0.23 (0.18–0.32) for S'TDI/SPAP. Mild aortic stenosis was diagnosed in 3.9% of cases, moderate in 9.2%, and severe in 3.9%.

Predictors of hospitalization for HF (Tables 3 and 4)

During a median follow-up of 391 days (84–704), 32% of patients (*n*=61) had at least one episode of HHF. In the univariate analysis, a higher TAPSE/SPAP ratio was associated with lower risk of HHF (HR 0.149; 95% CI 0.023–0.962; *p* = 0.039).

TAPSE (HR 0.959; 95% CI 0.921–0.998; *p* = 0.040) and age (for each year of increase: HR 1.066; 95% CI 1.015–1.120; *p* = 0.010) were also significant predictors, while SPAP did not reach statistical significance (HR 1.014; 95% CI 0.997–1.032; *p* = 0.100). The S'TDI/SPAP ratio showed no significant association in the univariate analysis (HR 0.096; 95% CI 0.00–24.33;

Table 1. Clinical population characteristics (n = 191)

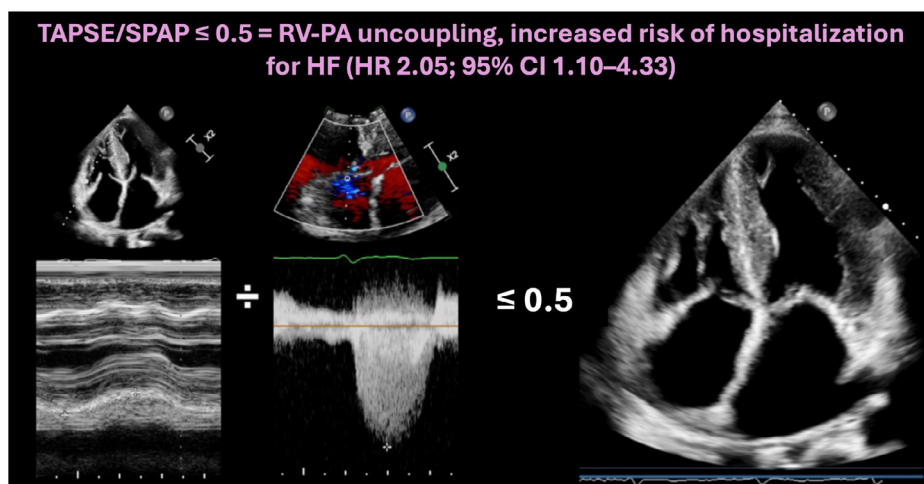
Variable	Value*
Male sex, n (%)	169 (88.5%)
Age, years, mean \pm SD	80 \pm 7.9 years
NYHA functional class 1, n (%)	62 (32.4%)
NYHA functional class 2, n (%)	100 (52.4%)
NYHA functional class 3, n (%)	28 (14.6%)
NYHA functional class 4, n (%) †	1 (0.52%)
Hypertension	131 (68.8%)
Dyslipidemia	104 (54.5%)
Diabetes	28 (14.6%)
Smoking	67 (35%)
Acute coronary syndrome	25 (13.1%)
Coronary angioplasty	41 (20.3%)
Myocardial revascularization surgery	16 (7.9%)
Valve replacement surgery	14 (6.9%)
Carpal tunnel syndrome	55 (27.2%)
Neuropathy	11 (5.4%)
Spinal stenosis	12 (5.9%)
Previous atrial fibrillation	93 (46.0%)
Atrial fibrillation in follow-up/development	26 (12.9%)
Previous cardiomyopathies	46 (22.8%)
Implantable cardioverter defibrillator	1 (0.5%)
Cardiac resynchronization therapy	2 (1.0%)

* Values are expressed as mean \pm SD, median (IQR), or n (%), as appropriate. NYHA functional class is that present at baseline TTE.

† One patient in NYHA class IV evaluated during hospitalization for HF was excluded.

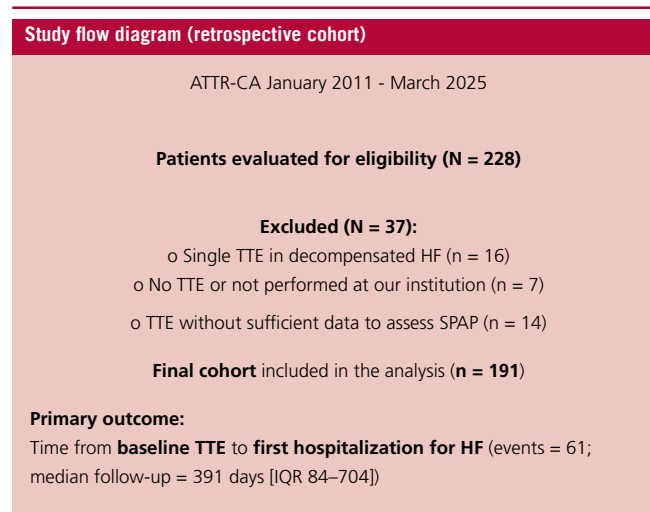
HF: heart failure; IQR: interquartile range; NYHA: New York Heart Association; SD: standard deviation; TTE: transthoracic echocardiogram

Central Figure. TAPSE/SPAP \leq 0.5 and risk of hospitalization for heart failure in CA-TTR.



Schematic illustration of right ventricle–pulmonary artery (RV–PA) uncoupling in transthyretin cardiac amyloidosis (ATTR-CA). A TAPSE/SPAP value \leq 0.5 identifies patients at higher risk of hospitalization for heart failure.

ATTR CA: transthyretin cardiac amyloidosis; HF: heart failure; RV-PA: right ventricle–pulmonary artery; SPAP: systolic pulmonary artery pressure; TAPSE: tricuspid annular plane systolic excursion.

Fig 1. Selection flow diagram for the ATTR-CA cohort

ATTR-CA: transthyretin cardiac amyloidosis; HF: heart failure; IQR: interquartile range; SPAP: systolic pulmonary artery pressure; TTE: transthoracic echocardiogram;

$p = 0.407$), with an unstable estimate due to a low proportion of censored cases and lower availability of measurements. Also, the age-adjusted S'TDI/SPAP ratio showed no independent association (HR 0.968; 95% CI 0.721–1.300; $p = 0.843$). Isolated RV S'TDI was also not associated with the outcome (HR 0.929; 95% CI 0.702–1.230; $p = 0.608$).

The AUC of the TAPSE/SPAP ratio for HHF was 0.60 (95% CI 0.50–0.71). The optimal cutoff point according to Youden's index was 0.5, with a sensitivity of 78% and specificity of 67%.

In the multivariate analysis, a TAPSE/SPAP ratio ≤ 0.5 was independently associated with a higher risk of HHF (HR 2.053; 95% CI 1.10–4.33; $p = 0.025$). Kaplan–Meier curves stratified by TAPSE/SPAP ≤ 0.5 showed consistent risk separation (log-rank in line with Cox model results (Figure 2).

DISCUSSION

In this contemporary cohort of ATTR-CA, the RV–PA uncoupling index derived from the TAPSE/SPAP ratio showed independent prognostic value of hospitalization for HF. We would like to highlight three main messages: (i) a TAPSE/SPAP ratio ≤ 0.50 identified a high-risk subgroup, with an association that persisted after adjustment; (ii) among the separate components, lower TAPSE and older age—but not SPAP alone—were associated with the outcome; and (iii) neither S'TDI nor S'TDI/SPAP provided prognostic value in this cohort. This pattern suggests that, in ATTR-CA, the interaction between RV contractility and afterload is better reflected by the TAPSE/SPAP ratio than by its components considered in isolation.

Relationship with previous evidence

The use of noninvasive indices of RV–PA uncoupling

for prognostic stratification was initially demonstrated in HF with preserved ejection fraction: in a large cohort, Guazzi et al. observed that TAPSE/SPAP < 0.35 was independently associated with the composite endpoint of HHF or death (27). Our findings are consistent in direction, although the optimal threshold was higher (0.50), a difference attributable to lower SPAP values.

In cardiac amyloidosis, studies in mixed AL and TTR cohorts showed that TAPSE/SPAP ratio predicts HHF and reported a mean TAPSE/SPAP value of ≈ 0.45 mm/mmHg as an independent predictor of death or HHF, (9) a finding subsequently confirmed in another smaller mixed cohort. (10)

Our work refines this evidence by focusing exclusively on ATTR-CA and evaluating multiple coupling indices. Even in a population mostly in early functional stages (85% NYHA \leq II), RV–PA uncoupling retained independent prognostic value, suggesting that poor RV adaptation to afterload may be an early phenomenon in the natural history of the disease, possibly favored by preferential infiltration of the basal RV segments. (28,29)

Pathophysiological interpretation

ATTR-CA combines myocardial stiffness and secondary pulmonary hypertension in advanced stages, conditions that strain RV–PA coupling. The TAPSE/SPAP ratio integrates, in a single measure, the longitudinal contractile reserve of the RV (TAPSE) and afterload (SPAP), capturing the mismatch between the two. The fact that the S'TDI (tissue velocity) parameter was not significant may reflect (i) its greater susceptibility to noise and angle, (ii) the basal segmental involvement of the RV typical of amyloidosis, and (iii) that, in this disease, small isolated decreases in longitudinal func-

Table 2. Baseline echocardiography and RV–PA indices (n = 191)

Parameter	Value
LVDD, mm, median (IQR)	44 (40–49)
LVSD, mm, median (IQR)	30 (25–35)
IVST, mm, median (IQR)	16 (14–19)
PWT, mm, median (IQR)	13 (12–15)
LVEF, %, median (IQR)	53 (43–61)
LA area, cm ² , median (IQR)	28 (25–33)
Mitral filling pattern (0–4)†	0: 2.6% 1: 13.9% 2: 25.2% 3: 23.2% 4: 35.1%
E/e', median (IQR)	14 (10–18)
Lateral S' (mitral), cm/s, median (IQR)	5 (4.3–6.5)
Septal S' (mitral), cm/s, median (IQR)	4 (0–5)
TAPSE, mm, median (IQR)	18 (15–20)
RV S'TDI, cm/s, median (IQR)	9.5 (8–10)
SPAP, mm Hg, median (IQR)	38 (31–48)
TAPSE/SPAP ratio, median (IQR)	0.43 (0.32–0.62)
RV S'TDI/SPAP ratio, median (IQR)	0.23 (0.18–0.32)
AoS	No: 82.9% Mild: 3.9% Moderate: 9.2% Severe: 3.9%

† Mitral filling pattern: 0 = normal; 1 = prolonged; 2 = pseudonormal; 3 = restrictive; 4 = monophasic wave.

AoS: aortic stenosis; E/e': mitral E wave to tissue e' ratio; IQR: interquartile range; IVST: interventricular septal thickness; LA: left atrium; lateral S' (mitral): systolic velocity of the lateral mitral annulus by tissue Doppler; LVDD: left ventricular diastolic diameter; LVEF: left ventricular ejection fraction; LVSD: left ventricular systolic diameter; PA: pulmonary artery; PWT: posterior wall thickness; RV: right ventricle; RV S'TDI: systolic velocity of the tricuspid annulus by tissue Doppler imaging; septal S' (mitral): systolic velocity of the septal mitral annulus by tissue Doppler imaging; SPAP: systolic pulmonary artery pressure; TAPSE: tricuspid annular plane systolic excursion

Table 3. Univariate analysis of predictors for heart failure hospitalization

Variable	HR	95% CI	p
TAPSE/SPAP (continuous)	0.149	0.023–0.962	0.039
TAPSE (mm)	0.959	0.921–0.998	0.040
Age (years)	1.066	1.015–1.120	0.010
SPAP (mmHg)	1.014	0.997–1.032	0.100
S'TDI (cm/s)	0.929	0.702–1.230	0.608
S'TDI/SPAP (continuous)	0.096	0.003–24.33	0.407

HR: hazard ratio; 95% CI: 95% confidence interval.

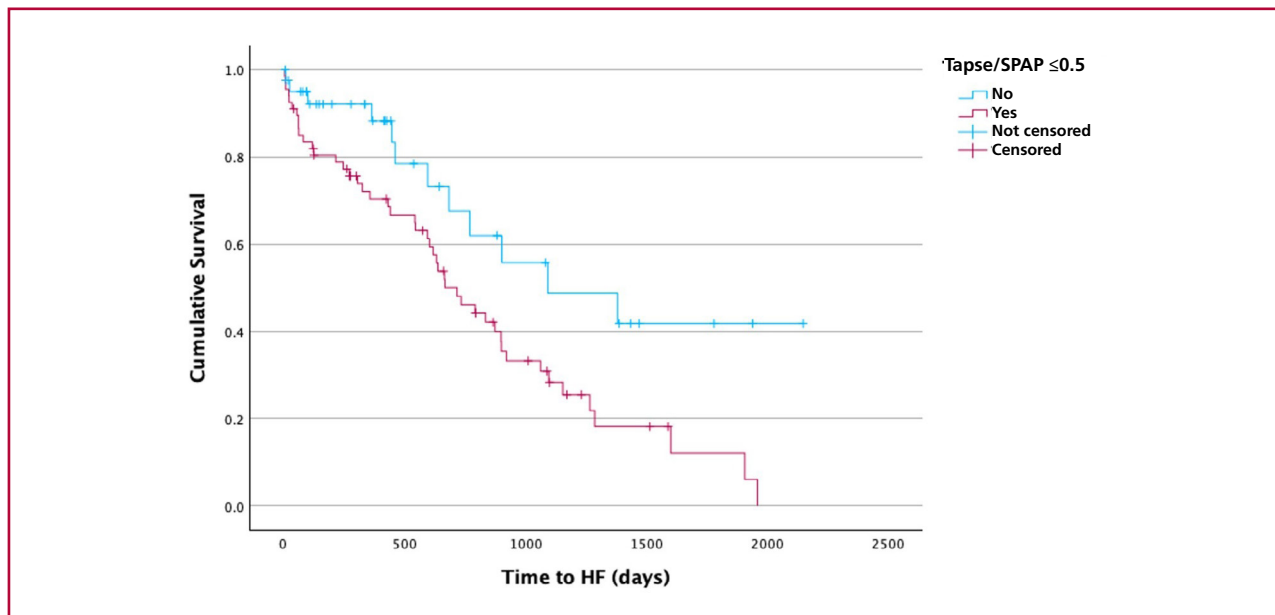
HF: heart failure; SPAP: systolic pulmonary artery pressure; S' TDI: S' wave by tissue Doppler imaging; TAPSE: tricuspid annular plane systolic excursion.

Table 4. Multivariate analysis of predictors for heart failure hospitalization.

Variable (model)	Adjusted HR	95% CI	p
TAPSE/SPAP \leq 0.50	2.053	1.10–4.33	0.025
S'TDI (cm/s) + age + SPAP	0.968	0.721–1.300	0.828
S'TDI/SPAP + age	0.101	0.00–30.92	0.432

HR: hazard ratio; 95% CI: 95% confidence interval.

SPAP: pulmonary artery systolic pressure; S' TDI: S' wave by tissue Doppler imaging; TAPSE: tricuspid annular plane systolic excursion.

Fig. 2. Kaplan–Meier curves according to TAPSE/SPAP

Heart failure hospitalization-free survival curves stratified according to TAPSE/SPAP cutoff point \leq 0.5. A significant separation of risks is observed (log-rank according to the Cox model).

HF: heart failure; SPAP: systolic pulmonary artery pressure; TAPSE: tricuspid annular plane systolic excursion.

tion might not translate into worse outcomes if they are not accompanied by elevated afterload. Taken together, this suggests that the contraction/afterload ratio provides more information than isolated "pieces" of RV mechanics.

Clinical implications

The TAPSE/SPAP index is simple, reproducible, and available in standard TTE. Its incorporation into baseline assessment could:

- Stratify risk and prioritize closer follow-up in patients with values \leq 0.50.
- Inform therapeutic decisions, favoring early optimization of HF management and timely evaluation of disease-modifying therapies when appropriate.
- Monitor trajectory: variations in TAPSE/SPAP over time could signal progression ("dynamic" uncoupling).

This index should complement, not replace, multiparametric assessment with biomarkers, functional class, LV parameters, and, when available, RV free wall strain.

LIMITATIONS

The observational, retrospective, and single-center design implies a risk of selection bias. In addition, the estimation of SPAP by Doppler may introduce errors related to the tricuspid regurgitation signal and the estimation of right atrial pressure. Right ventricular strain indices and invasive hemodynamic measurements, which would have allowed the calculation of elastances, were not systematically incorporated. The primary outcome considered was the first HHF, excluding mortality and composite outcomes, which may limit comparison with other series. Finally, the cohort spanned several years, during which the management of ATTR-CA was modified, introducing a possible treatment-related confounding factor.

CONCLUSIONS

In this cohort of ATTR-CA with preserved LVEF, RV-PA uncoupling measured by TAPSE/SPAP was independently associated with an increased risk of first

hospitalization for HF, identifying a practical threshold (≤ 0.50) with potential clinical utility. In contrast, strain-based indices showed no independent association with the outcome.

Prospective, multicenter studies are warranted to: (i) externally validate the cutoff point ≤ 0.50 ; (ii) evaluate the incremental value of TAPSE/SPAP over clinical models and biomarkers; (iii) compare its performance with S'TDI and S'TDI/SPAP; (iv) analyze its longitudinal evolution and modulation by specific therapies; and (v) consider hard endpoints and phenotypic subgroups.

Conflicts of interest

None declared.

(See authors' conflict of interests forms on the web).

REFERENCES

- Wechalekar AD, Gillmore JD, Hawkins PN. Systemic amyloidosis. *Lancet* 2016;387:2641-54. [https://doi.org/10.1016/S0140-6736\(15\)01274-X](https://doi.org/10.1016/S0140-6736(15)01274-X)
- Fontana M, Ćorović A, Scully P, Moon JC. Myocardial amyloidosis: the exemplar interstitial disease. *JACC Cardiovasc Imaging* 2019;12:2345-56. <https://doi.org/10.1016/j.jcmg.2019.06.023>
- Quarta CC, Kruger JL, Falk RH. Cardiac amyloidosis. *Circulation* 2012;126:e178-82. <https://doi.org/10.1161/CIRCULATIONAHA.111.069195>
- Garcia-Pavia P, Rapezzi C, Adler Y, Arad M, Basso C, Brucato A, et al. Diagnosis and treatment of cardiac amyloidosis: a position statement of the ESC Working Group on Myocardial and Pericardial Diseases. *Eur Heart J* 2021;42:1554-68. <https://doi.org/10.1093/eurheartj/ehab072>
- Maccallini M, Barge-Caballero G, Barge-Caballero E, López-Pérez M, Bilbao-Quesada R, González-Babarro E, et al. Prognostic value of the tricuspid annular plane systolic excursion/systolic pulmonary artery pressure ratio in cardiac amyloidosis. *Rev Esp Cardiol* 2024;77:634-44. <https://doi.org/10.1016/j.recresp.2024.01.001>
- de Groote P, Fertin M, Goéminne C, Petyt G, Peyrot S, Foucher-Hossein C, et al. Right ventricular systolic function for risk stratification in patients with stable left ventricular systolic dysfunction: comparison of radionuclide angiography to echoDoppler parameters. *Eur Heart J* 2012;33:2672-9. <https://doi.org/10.1093/eurheartj/ehs080>
- Naseem M, Alkassab A, Alaarag A. Tricuspid annular plane systolic excursion/pulmonary arterial systolic pressure ratio as a predictor of in-hospital mortality for acute heart failure. *BMC Cardiovasc Disord* 2022;22:414. <https://doi.org/10.1186/s12872-022-02857-6>
- Yu F, Cui Y, Shi J, Wang L, Zhou Y, Ye T, et al. Association between the TAPSE to SPAP ratio and short-term outcome in patients with light-chain cardiac amyloidosis. *Int J Cardiol* 2023;387:131108. <https://doi.org/10.1016/j.ijcard.2023.05.058>
- Tomasoni D, Adamo M, Porcari A, Aimo A, Bonfili GB, Castiglione V, et al. Right ventricular to pulmonary artery coupling and outcome in patients with cardiac amyloidosis. *Eur Heart J Cardiovasc Imaging* 2023;24:1405-14. <https://doi.org/10.1093/ehjci/jead145>
- Palmiero G, Monda E, Verrillo F, Calabrò P, Bossone E, Limongelli G, et al. Prevalence and clinical significance of right ventricular pulmonary arterial uncoupling in cardiac amyloidosis. *Int J Cardiol* 2023;388:131147. <https://doi.org/10.1016/j.ijcard.2023.131147>
- Pestelli G, Fiorencis A, Trevisan F, Luisi GA, Smarrazzo V, Mele D. New measures of right ventricle-pulmonary artery coupling in heart failure: an all-cause mortality echocardiographic study. *Int J Cardiol* 2021;329:234-41. <https://doi.org/10.1016/j.ijcard.2020.12.057>
- Guazzi M, Bandera F, Pelissero G, Castelvechio S, Menicanti L, Ghio S, et al. Tricuspid annular plane systolic excursion and pulmonary arterial systolic pressure relationship in heart failure: an index of right ventricular contractile function and prognosis. *Am J Physiol Heart Circ Physiol* 2013;305:H1373-81. <https://doi.org/10.1152/ajpheart.00157.2013>
- Bosch L, Lam CSP, Gong L, Chan SP, Sim D, Yeo D, et al. Right ventricular dysfunction in left-sided heart failure with preserved versus reduced ejection fraction. *Eur J Heart Fail* 2017;19:1521-31. <https://doi.org/10.1002/ejhf.873>
- Kittleson MM, Maurer MS, Ambardekar AV, Bullock-Palmer RP, Chang PP, Eisen HJ, et al. Cardiac amyloidosis: evolving diagnosis and management: a scientific statement from the American Heart Association. *J Am Heart Assoc* 2020;9:e017905. <https://doi.org/10.1161/CIR.0000000000000792>
- Trousselle L, Eggenspiepler F, Huttin O, Pace N, Nazeyrollas P, Faroux L, et al. Echocardiographic assessment of right ventricular function and right ventriculoarterial coupling in tricuspid regurgitation. *Int J Cardiovasc Imaging* 2024;40:2247-59. <https://doi.org/10.1007/s10554-024-03215-7>
- Roccabruna A, Fortuni F, Comuzzi A, Armani I, Bolzan B, Franchi E, et al. Right ventricular-pulmonary artery coupling in patients undergoing cardiac resynchronization therapy. *Int J Cardiovasc Imaging* 2024;40:2325-34. <https://doi.org/10.1007/s10554-024-03233-5>
- Lillo R, Graziani F, Ingrassiotta G, Przybylsek B, Iannaccone G, Locorotondo G, et al. Right ventricle systolic function and right ventricle-pulmonary artery coupling in patients with severe aortic stenosis and the early impact of TAVI. *Int J Cardiovasc Imaging* 2022;38:1761-70. <https://doi.org/10.1007/s10554-022-02569-0>
- Schwartz SK, Poledniczek M, Metodieff Y, Stolz L, Hofmann E, Hegenbart U, et al. RV-PA uncoupling is associated with increased mortality in transthyretin amyloid cardiomyopathy treated with tafamidis. *Clin Res Cardiol* 2024;113. <https://doi.org/10.1007/s00392-024-02576-2>
- Kittleson MM, Ruberg FL, Maurer MS, Ambardekar AV, Bullock-Palmer RP, Chang PP, et al. 2023 ACC Expert Consensus Decision Pathway on Comprehensive Multidisciplinary Care for the Patient With Cardiac Amyloidosis: a report of the American College of Cardiology Solution Set Oversight Committee. *J Am Coll Cardiol* 2023;81:1076-126. <https://doi.org/10.1016/j.jacc.2022.11.022>
- Rudski LG, Lai WW, Afilalo J, Hua L, Handschumacher MD, Chandrasekaran K, et al. Guidelines for the echocardiographic assessment of the right heart in adults: a report from the American Society of Echocardiography. *J Am Soc Echocardiogr* 2010;23:685-713. <https://doi.org/10.1016/j.echo.2010.05.010>
- Gillmore JD, Maurer MS, Falk RH, Merlini G, Damy T, Dispenzieri A, et al. Nonbiopsy diagnosis of cardiac transthyretin amyloidosis. *Circulation* 2016;133:2404-12. <https://doi.org/10.1161/CIRCULATIONAHA.116.021612>
- Konstam MA, Kiernan MS, Bernstein D, Bozkurt B, Jacob M, Kapur NK, et al. Evaluation and management of right-sided heart failure: a scientific statement from the American Heart Association. *Circulation* 2018;137:e578-622. <https://doi.org/10.1161/CIR.0000000000000560>
- Cappelli F, Porciani MC, Bergesio F, Perlini S, Attanà P, Moggi Pignone A, et al. Right ventricular function in AL amyloidosis: characteristics and prognostic implication. *Eur Heart J Cardiovasc Imaging* 2012;13:416-22. <https://doi.org/10.1093/ejehoccard/jer289>
- Lang RM, Badano LP, Mor-Avi V, Afilalo J, Armstrong A, Ernande L, et al. Recommendations for cardiac chamber quantification by echocardiography in adults: an update from the American Society of Echocardiography and the European Association of Cardiovascular Imaging. *J Am Soc Echocardiogr* 2015;28:1-39. <https://doi.org/10.1016/j.echo.2014.10.003>
- Badano LP, Kolias TJ, Muraru D, Abraham TP, Aurigemma G, Edvardsen T, et al. Standardization of left atrial, right ventricular, and right atrial deformation imaging using two-dimensional

speckle tracking echocardiography: a consensus document of the EACVI/ASE/Industry Task Force to standardize deformation imaging. *Eur Heart J Cardiovasc Imaging* 2018;19:591-600. <https://doi.org/10.1093/ehjci/jey042>

26. World Medical Association. World Medical Association Declaration of Helsinki: Ethical Principles for Medical Research Involving Human Subjects. *JAMA* 2013;310:2191-4. <https://doi.org/10.1001/jama.2013.281053>

27. Guazzi M, Dixon D, Labate V, Beussink-Nelson L, Bandera F, Cuttica MJ, et al. RV contractile function and its coupling to pulmonary circulation in heart failure with preserved ejection fraction: stratification of clinical phenotypes and outcomes. *JACC Cardiovasc Imaging*. 2017;10:1211-21. <https://doi.org/10.1016/j.jcmg.2016.12.024>

28. De Gaspari M, Sinigiani G, De Michieli L, Della Barbera M, Rizzo S, Thiene G, et al. Relative apical sparing in cardiac amyloidosis is not always explained by an amyloid gradient. *Eur Heart J Cardiovasc Imaging*. 2023;24:1258-68. <https://doi.org/10.1093/ehjci/jead107>

29. Porcari A, Fontana M, Canepa M, Biagini E, Cappelli F, Gagliardi C, et al. Clinical and prognostic implications of right ventricular uptake on bone scintigraphy in transthyretin amyloid cardiomyopathy. *Circulation* 2024;149:1157-68. <https://doi.org/10.1161/CIRCULATIONAHA.123.066524>